INFLUENCE OF THE ANGULAR CONTACT IN THE KINEMATIC AND DYNAMIC ANALYSIS OF ROLLING ELEMENT BEARINGS

Rafael Vischi Carvalho, rvischi@gmail.com
Schaeffler Brasil Ltda, Av. Independencia, 3500, Sorocaba, SP, Brazil, e-mail: carvaraf@schaeffler.com

Katia Lucchesi Cavalca Dedini, katia@fem.unicamp.br
University of Campinas, Faculty of Mecanical Engineering, Postal Box 6122, Campinas, SP, Brazil, e-mail: kátia@fem.unicamp.br

Abstract. *Ball bearings are common machine elements but largely used in several applications involving high velocities, high temperatures and different loads. The load model is fundamental for the ball bearing's dynamic and for this reason it is necessary to accurately define the mechanisms performance using analytical methods. The objective of this paper is to study the ball bearings, firstly, regarding to the theory involved in the kinematic and dynamic modeling. Afterwards, the model developed to the numerical simulations is analyzed regarding to the influences due to the gyroscopic moment and the relative velocities, due to the bearing's components relative motion, on the load distribution on the bearing. Considering a commercial and well-known rolling element bearing, numerical simulation tests were accomplished, varying the main critical design parameters of these elements to study their effects on the kinematic, dynamic and static behavior of the angular contact ball bearing. The results show that the angular velocity and the contact angle have influence on the friction forces that resist to the gyroscopic moment and also on the velocities that are generated at the contact zones between the sphere and both inner and outer raceways. Under certain rotation speeds, particular kinematic and dynamic conditions can occur, such as higher the value of the rotation speed is, higher is the influence on the precession and nutation angles, causing sliding motion at the contact area. The nutation angle corresponding to the null angular velocity normal to the contact plane was verified, validating the outer raceway control condition. The analytical model results were satisfactorily consistent with the classical literature approaches and also with some experimental tests accomplished by rolling bearings manufacturers. The kinematic and dynamic models are promising to estimate the expected behavior for the relative velocities, angular velocities and accelerations, as well as the load distribution commonly present in the rolling element. These factors are highly related to the lubrication condition at the contact region between the rolling element and the bearing raceways.*

Keywords*: Rolling element bearings, gyroscopic moment, relative motion, load distribution.*

1. INTRODUCTION

For a ball bearing's more realistic simulation, an elastohydrodynamic model is needed as the oil film cannot be predicted by the hydrodynamic lubrication theory due to the limitations in considering high loads and stresses at the contact area. The elastohydrodynamic (EHD) lubrication theory studies the interaction of the components elasticity in contact considering the oil film within the interfaces. The elasticity of the bodies in contact directly influences the lubrication condition. When the bodies are deformed due to the contact stresses, there is a better geometric conformation between them, and consequently, the oil film thickness depends on the new condition of gap between these bodies. In ball bearings, the oil film is theoretically formed in the contact point between the sphere and the raceways, which have different curvature radius. To better know the EHD lubrication effects, firstly, it is necessary to deeply understand the forces and loads applied in the ball bearing. The main objective of this work is to analyze the ball bearing using dynamic and kinematic techniques.

Deeper studies involving rolling element bearings have been developed since 1900. Goodman (1912) published his equations, based on fatigue data, for the load distribution calculation from bearings.

The published book, *Rolling Bearing Analysis* (HARRIS, 1991), detailed described a rolling element bearing, its main applications and all the engineering and technical development behind the system. Harris and Kotzalas (2006) also published the book *Advanced Concepts of Bearing Technology*, where a more complex analysis of the dynamic and kinematic involved in a ball bearing is discussed.

Changsen (1991), a classical author in this field, studied in his book the ball bearing's dynamic model. He discussed and presented the Hertz theory, the bearing kinematic and the load distribution.

Gupta (1979) presented a simulation of a generic sphere, retainer and raceway in a ball bearing by differential equations, in a sophisticated mathematical representation.

Later, Meeks and Tran (1996) developed a theoretical dynamic analysis for a six degree of freedom system, where complete kinematic and dynamic effects were modeled.

Hagiu (1997) studied the damping and stiffness of a contact angle bearing under high rotation, used for grinding machines. Recently, Changqing (2006) presented a generic model to study the dynamic properties of a rotor, which is supported by ball bearings that present gap and waviness in the raceways. At the simulation, the effects of rotation and

normal forces at the contact area were included. The results showed that the gap, the preload and the load are highly significant for the system's stability.

In *Ball bearing skidding under radial and axial loads* (LIAO, 2002), a ball bearing under high rotation was submitted to axial and radial loads to investigate the radial force effect. Applying a equilibrium analysis, several parameters were obtained: normal forces, contact angle at the outer raceway and axial and radial displacement.

In this context, this paper contributes for the characterization and determination of the loads involved at a ball bearing. The results will be used later for the analysis of the EHD lubrication condition.

2. THEORETICAL MODEL

Figure 1 introduces the problem of a contact angle ball bearing, the contact area between sphere and raceways, as well as the main loads that are applied to the bearing and also to the spheres. A radial load Q_r is transmitted from the outer ring to each sphere, and then decomposed at the contact area in a normal load Q and a tangential load Q_t. The normal force occurs at the contact point due to the trajectory curvature and the rotation velocity of the sphere, which moves towards the external raceway, causing different contact angles in the inner (α_i) and outer (α_o) raceways. At this condition, a new equilibrium position must be reached, which is highly associated to the contact local deformation. Therefore, all the equilibrium mechanism has a considerable influence over the EHD lubrication condition.

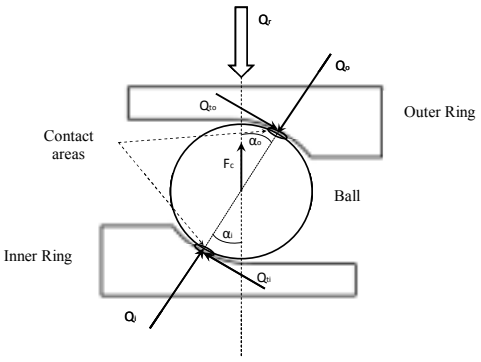

Figure 1: Load condition in a contact angle ball bearing.

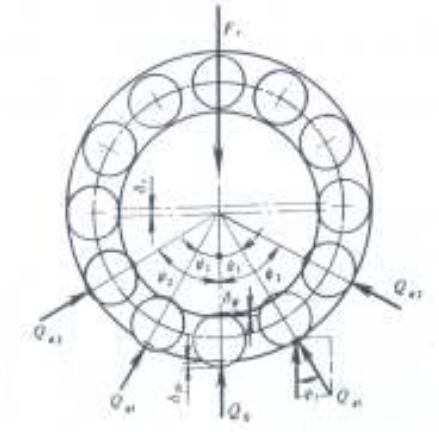

Figure 2: Load distribution in radial bearings (CHANGSEN, 1991)

2.1 Radial Load

Figure 2 shows the load distribution at radial bearings (contact angle α = 0) with null clearance, a desirable condition for practical applications. The parameter (ψ) is defined as the angular position between the line of action that contains the total external applied force (F_r) and the line passing through the bearing center and each sphere center, called the Azimuth angle. Q_ψ is the load applied at each rolling element at ψ_t position, δ_r is the relative radial displacement and δ_ψ is the total displacement at the ψ angle (δ_0 is the total displacement at $\psi = 0$, or $\delta_0 = \delta_{max}$). For the bearing showed in Figure 2, the static equilibrium condition at the inner raceway is given by Equation (1):

$$F_r = Q_0 + 2\sum Q_\psi \cos\psi \tag{1}$$

Consequently, the total elastic displacement (δ_ψ), at the Azimuth angle ψ, for a null clearance, is given by Equation (2):

$$\delta_\psi = \delta_r \cos\psi = \delta_{max} \cos\psi \tag{2}$$

Considering the same radial bearing with a positive diametral clearance P_d and developing Equation 2, the final expression for the total elastic displacement (δ_ψ) is obtained. (CHANGSEN, 1991):

$$\delta_\psi = \delta_{\max}\left[1-\frac{1}{2\varepsilon}(1-\cos\psi)\right]$$
$$\varepsilon = \frac{1}{2}\left(1-\frac{P_d}{2\delta_r}\right) \tag{3}$$

Therefore, for a generic contact, the load for each rolling element can be defined as:

$$Q_\psi = Q_{\max}\left[1-\frac{1}{2\varepsilon}(1-\cos\psi)\right]^n \tag{4}$$

Q_ψ is the load at Azimuth position ψ and Q_{max} is the load for the maximum elastic displacement δ_{max}.

In this case, applying the eq. (1) of static equilibrium for radial bearings, the outer radial load must be equal to the sum of the vertical components of the loads acting at the spheres.

$$F_r = Q_{\max}\sum_{\psi=0}^{\psi=\pm 1}\left[1-\frac{1}{2\varepsilon}(1-\cos\psi)\right]^n \cos\psi \tag{5}$$

Equation (5) evaluates the loads and their distribution on the rolling elements. At this condition, it will be added the kinematic and dynamic effects due to the contact angle and radial acceleration for high rotations, which will be studied next.

2.2 Kinematic Analysis

The components of the rotation velocities are fundamental for the study of the forces involved in the load distribution. Hence, it is necessary to establish the angular and linear velocities of the components of the bearing: inner and outer raceways, retainer, and rolling elements or spheres. Besides, for a deeper study at the contact area, an analysis of the relative motion between inner and outer raceways and the rolling element is necessary to define the normal angular velocity at the contact, well known as spinning effect.

The kinematic relations are under the following statements: a) all the bearing elements are rigid; b) the rolling elements motion at the raceways are considered pure rolling; c) the radial clearance influence is not considered at the rotation velocities; d) the EHD lubrication effect is not taken into account.

Figure 3 shows a contact angle bearing and the main rotations involved at the inner raceway (n_i), the outer raceway (n_o), the retainer (n_m) and the rolling elements (n_R).

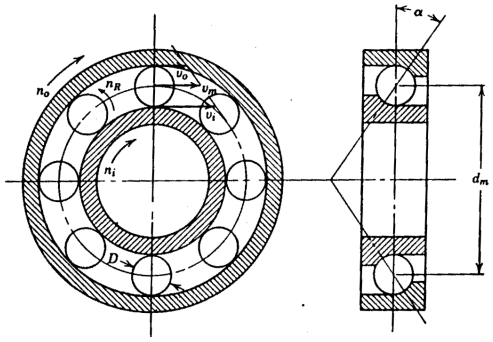

Figure 3: Main rotation speeds (HARRIS and KOTZALAS, 2006)

The evaluation of the sphere rotation velocity (n_R) depends on the retainer rotation velocity (n_m), which is related to the rotations of the inner (n_i) and outer (n_o) raceways. (CHANGSEN, 1991; HARRIS, 2006):

$$n_m = 1/2\ [n_i\ (1 - \gamma) + n_0\ (1 + \gamma)] \tag{6}$$

where $\gamma = (D\cos\alpha)/d_m$

$$n_R = d_m/2D\ [(1 - \gamma)(n_0 - n_i)(1 + \gamma)] \tag{7}$$

From Equations (6) and (7), D is the sphere diameter, d_m is the pitch diameter and α is the contact angle of the sphere (Figure 3). Therefore, the effect due to the normal acceleration can be included at the dynamic model.

2.3 Normal Force On the Sphere

To calculate the normal force acting at the contact area, the angular velocity in which the sphere orbits around the rotational axis of the bearing ($\omega_m = 2\pi(n_m)/60$) is considered. The normal force is given by the Newton' law, depending on the mass of the sphere m and the radial acceleration a_c:

$$m = \frac{1}{6}\rho\pi D^3$$
$$a_c = \frac{d_m \omega_m^{\,2}}{2} \tag{8}$$
$$F_{z'} = \frac{1}{12}\rho\pi D^3 d_m \omega_m^{\,2}$$

2.4 Kinematic Analysis at the Contact Areas

Figure 4 shows the contact between the rolling element and the outer raceway, where the normal force is distributed over an elliptical surface that represents the contact area. The ellipse major and minor semi axes are denominated by a_0 e b_0 respectively. The curvature radius of the deformed pressured region (R_0) is defined by Hertz (HARRIS and KOTZALAS, 2006; NONATO, 2009).

To analyze the kinematic condition at the contact, the relative motion must be described at the rolling element's reference, which means, it is assumed that the sphere center is fixed in the space and that the outer raceway is turning around it with angular velocity ω_0 that is collinear to the bearing's rotation axis. This assumption allows the analysis of any sphere independently of its position angle ψ (Azimuth) in the bearing. Therefore, the outer ring velocity relative to the sphere center is given by:

$$\omega_0 = \frac{\omega_R D}{D + d_m} \tag{9}$$

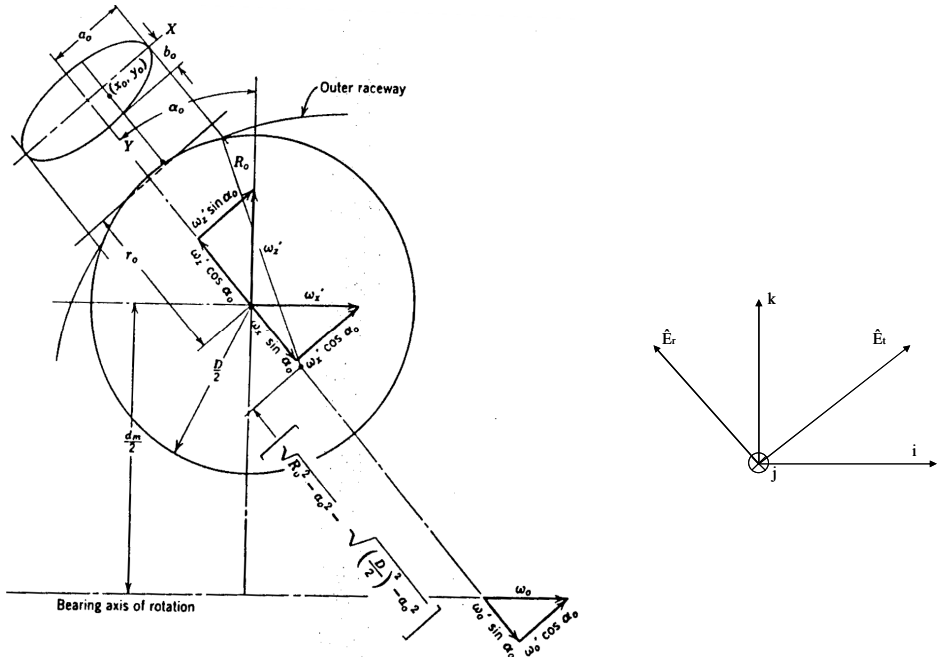

Figure 4: Contact between ball and outer raceway (HARRIS, 2006)

The sphere rotation (ω_R) components $\omega_{x'}$ e $\omega_{z'}$ at the sphere local reference system are shown in Figure 4.

Considering the imaginary line that connects the sphere center to the center of the contact area, perpendicular to the sphere rotation axis, the outer raceway has a component $\omega_0 cos\alpha_0$, vector projection of the angular velocity (ω_0) in the sphere angular velocity direction, which is parallel to the contact ellipse minor axis in y direction.

The tangential velocity at the outer raceway surface (v_{10}) is the sum of the raceway velocity at the contact, in relation to the sphere center, and its translation velocity in the bearing reference (-(dmω_0)/2). Besides, the tangential velocity at the contact area is obtained by the vectorial product between the distance from the sphere center to the contact point, and the projection of the raceway angular velocity at the sphere local referential ($\omega_0 cos\alpha_0$). Therefore, for a generic point (x_0,y_0) at the contact region of the outer raceway, the tangential velocity v_{10} is defined as:

$$v_{10} = \left(-\frac{d_m \omega_0}{2} - \left\{ \left(R_0^{\,2} - x_0^{\,2} \right)^{1/2} - \left(R_0^{\,2} - a_0^{\,2} \right)^{1/2} + \left[\left(\frac{D}{2} \right)^2 - a_0^{\,2} \right]^{1/2} \right\} \omega_0 \cos\alpha_0 \right) j \tag{10}$$

The vector projection of the sphere angular velocities, regarding the contact angle (α_0) gives the components $\omega_{x'} cos\alpha_0$ e $\omega_{z'} sin\alpha_0$, also parallel to the major contact ellipse axis in Figure 4. For the point (x_0,y_0), now located at the ball surface, the linear velocity v_{20} is defined in relation to the sphere center as:

$$v_{20} = \left(-\left(\omega_{x'} \cos\alpha_0 + \omega_{z'} \sin\alpha_0 \right) \times \left\{ \left(R_0^{\,2} - x_0^{\,2} \right)^{1/2} - \left(R_0^{\,2} - a_0^{\,2} \right)^{1/2} + \left[\left(\frac{D}{2} \right)^2 - a_0^{\,2} \right]^{1/2} \right\} \right) j \tag{11}$$

The sliding velocity at the outer raceway contact point in y direction, as shown in Figure 4, is determined by the difference between the tangential velocities given in Equations (10) and (11):

$$v_{y0} = v_{10} - v_{20}$$

$$v_{y0} = \left(-\frac{d_m \omega_0}{2} + \left(\omega_{x'} \cos\alpha_0 + \omega_{z'} \sin\alpha_0 - \omega_0 \cos\alpha_0 \right) x \right.$$

$$\left. v_{y0} = \left\{ \left(R_0^{\,2} - x_0^{\,2} \right)^{1/2} - \left(R_0^{\,2} - a_0^{\,2} \right)^{1/2} + \left[\left(\frac{D}{2} \right)^2 - a_0^{\,2} \right]^{1/2} \right\} \right) j \tag{12}$$

Additionally, the sphere angular velocity (ω_R) has a component $\omega_{y'}$, responsible for the sliding velocity of the outer raceway in the x direction, or parallel to the major contact ellipse axis. The v_{x0} can be written as:

$$v_{x0} = \left(-\omega_{y'} \left\{ \left(R_0^{\,2} - x_0^{\,2} \right)^{1/2} - \left(R_0^{\,2} - a_0^{\,2} \right)^{1/2} + \left[\left(\frac{D}{2} \right)^2 - a_0^{\,2} \right]^{1/2} \right\} \right) i \tag{13}$$

Both components ($\omega_{x'}$ e $\omega_{z'}$) of the sphere angular velocity, as well as the outer raceway angular velocity ω_0, present projections $\omega_{x'} sin\alpha_0$ e $\omega_{z'} cos\alpha_0$ (sphere) and $\omega_0 sin\alpha_0$ (raceway) as shown in Figure 4. All these vector components are normal to the contact region, causing a relative rotation sphere-raceway, called spinning (ω_{s0}).

$$\omega_{s0} = \left(\left(\omega_{x'} \sin\alpha_0 - \omega_{z'} \cos\alpha_0 \right) - \omega_0 \sin\alpha_0 \right) \hat{E}r \tag{14}$$

Figures 5(a) and 5(b) shows the vector components of the sphere angular velocity (ω_R) at the coordinate system x'y'z', with fixed center at the sphere geometric center, represented by $\omega_{x'}$, $\omega_{y'}$ e $\omega_{z'}$ and according the following definition: xyz is the fixed coordinated system with x axis coincident to the bearing rotation axis; x'y'z' is the sphere local coordinated system with x' parallel to x, that turns around the x axis; ψ is the sphere position angle (Azimuth), or else the angle between z e z' axes; β is the angle between the sphere rotation velocity vector (ω_R) and the x'y' plane; β' is the angle between ω_R projection at the x'y' plane and the x' axis.

From Figure 5, the ω_R components at x'y'z' are obtained, which are replaced in equations (12), (13) and (14):

$$\begin{aligned} \omega_{x'} &= \left(\omega_R \cos\beta \cos\beta' \right) i \\ \omega_{y'} &= \left(\omega_R \cos\beta sen\beta' \right) j \\ \omega_{z'} &= \left(\omega_R sen\beta \right) k \end{aligned} \tag{15}$$

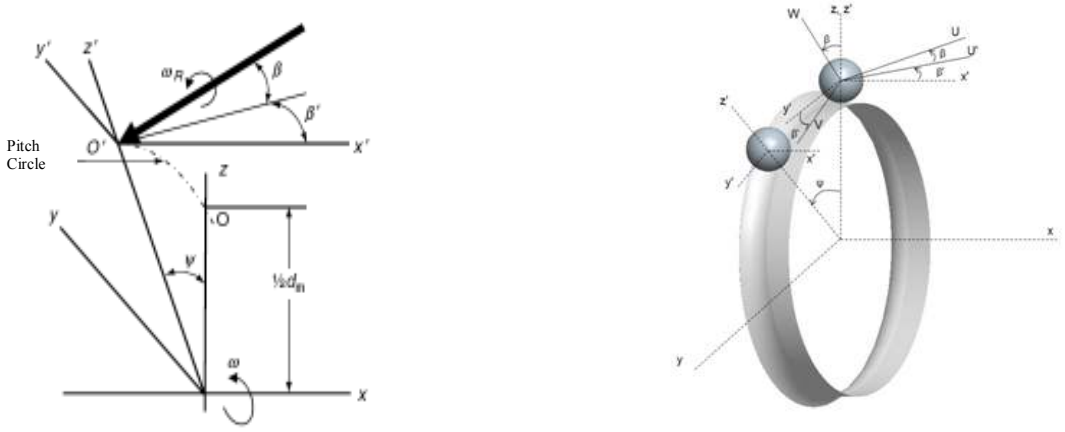

(a) (b)

Figure 5: Coordinated system at the sphere (rolling element) and at the bearing (HARRIS, 2006)

Considering a pure rolling radius r_0' in which the sphere translation velocity is identical to the outer raceway one:

$$\left(\frac{d_m}{2\cos\alpha_0}+r_0'\right)\omega_0\cos\alpha_0 = r_0'\left(\omega_{x'}\cos\alpha_0+\omega_{z'}\sin\alpha_0\right)$$
$$\left(\frac{d_m}{2\cos\alpha_0}+r_0'\right)\omega_0\cos\alpha_0 = r_0'\left(\omega_R\cos\beta\cos\beta'\cos\alpha_0+\omega_R sen\beta\sin\alpha_0\right) \quad (16)$$
$$\frac{\omega_R}{\omega_0} = \frac{\left(d_m/2\right)+r_0'\cos\alpha_0}{r_0'\left(\cos\beta\cos\beta'\cos\alpha_0+\sin\beta\sin\alpha_0\right)}$$

A similar analysis can be applied to the inner raceway contact, assuming that the outer raceway is fixed. Then, the sphere center can orbit around the fixed reference system at the bearing with rotation $-\omega_0$.

Investigating the final equations, associated to the relative motion between sphere and raceways, the following information is required: r_0', r_i', α_0, α_i, β, β'.

The sphere pure rolling radii relative to both outer and inner raceways (r_0' and r_i'), can be approached by the sphere radius ($D/2$). For the sake of simplicity, the special case where the sphere (rolling element) angular velocity (ω_R) is located at the x'z' plane, the β' angle is null in Figure 5, focusing then on the effect of the β component of the nutation angle, which direction is coincident with the bearing contact angle (α). Finally, the design hypothesis of the sphere pure rolling over one of the raceways is applied, without sliding or spinning. When considered at the outer raceway, this hypothesis goes towards the principle established by Jones (1960), called outer raceway control.

In lubricated contact angular bearings operating, at high rotations and low loads, the normal angular velocity at sphere – outer raceway contact is practically zero (HARRIS and KOTZALAS, 2006), working closer to the outer raceway control condition. It is also a fact that the contact angle increases the axial load at the bearing, minimizing the spinning effect at the outer raceway contact when compared to the inner raceway.

Replacing Equation (15) in Equation (14):

$$\omega_{s0} = \left(\left(\frac{\omega_R}{\omega_0}\cos\beta\cos\beta'\sin\alpha_0 - \frac{\omega_R}{\omega_0}sen\beta\cos\alpha_0 - \sin\alpha_0\right)\omega_0\right)\hat{E}r \quad (17)$$

Applying $\beta' = 0$ and the outer raceway control condition ($\omega_{s0} = 0$) in Equation (17), and with Equation (16), the nutation angle β can be defined:

$$tg\beta = \frac{d_m sen\alpha_0}{D + d_m\cos\alpha_0} \quad (18)$$

Equation (18) gives the nutation angle β regarding the bearing design parameters (sphere diameter, bearing pitch diameter and contact angle) for the outer raceway control condition.

3 RESULTS AND DISCUSSIONS

3.1 Static analysis: radial load distribution

Figures 6 and 7 present the radial load distribution considering null diametral clearance and also the effect of the inner raceway rotation velocity on the load distribution due to the radial force.

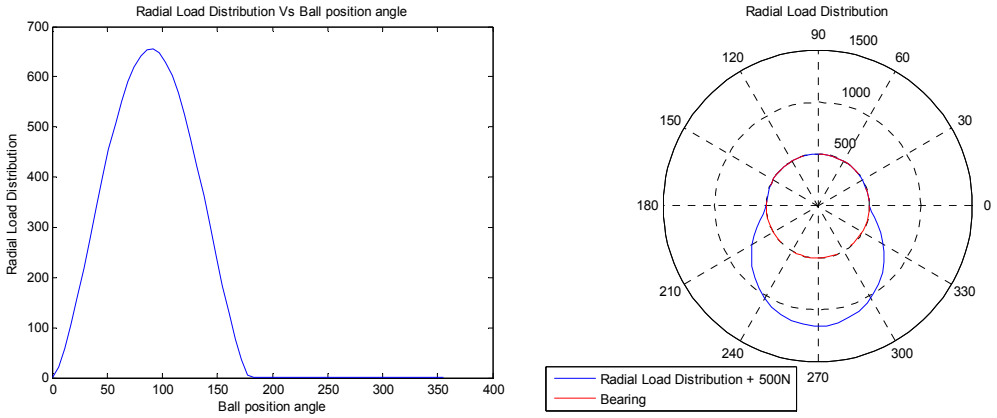

Figure 6: Radial load distribution in function of the ball contact angle at 2000 rpm – $P_d = 0$

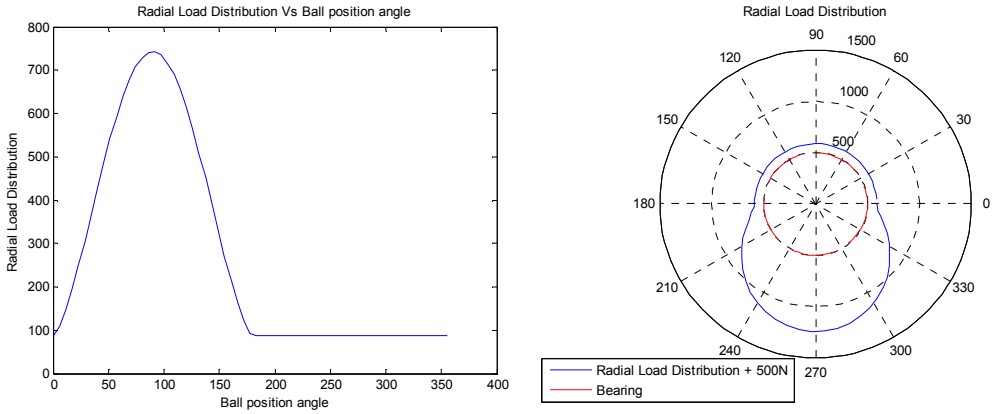

Figure 7: Radial load distribution in function of the ball contact angle at 50000 rpm – $P_d = 0$

It is observed that at high rotations, the radial force effect in all rolling elements is even more expressive and its contribution is added to the static force distribution due to the external load.

3.2 Kinematic analysis

Figures 8 to 10 show the kinematic analysis results. Figures 8(a) and 8(b) show the spinning (normal angular velocity) generated at the contact areas with the outer (ω_{so}) and the inner (ω_{si}) raceways, depending on the inner raceway rotation (n_i) and the bearing contact angle (α). Figures 9(a) and 9(b) show the influence of the same factors (n_i and α) on the sliding velocity at the outer raceway in y direction (v_{oy}) at the center ($x_0 = 0$) and the extreme ($x_0 = a_0$) points of the contact region. Analogously, Figures 10(a) and 10(b) show the sliding velocities at the inner raceway (v_{iy}).

According figures 8(a) and 8(b), the angular velocity, normal to the contact surface (spinning), at the inner raceway, is highest than at the outer raceway, according to the outer raceway control design condition.

Considering the inner raceway rotation (n_i) of 50.000 rpm, the sphere surface tangential velocity is close to 44,45 m/s. In this case, the outer raceway sliding is approximately 1,75 m/s at the contact center, and 2,1 m/s at the extremity (Figures 9(a) and 9(b)). Considering the inner raceway rotation of 10.000 rpm, an usual rotation in several applications, the outer raceway sliding is almost zero, in agreement with the outer raceway control.

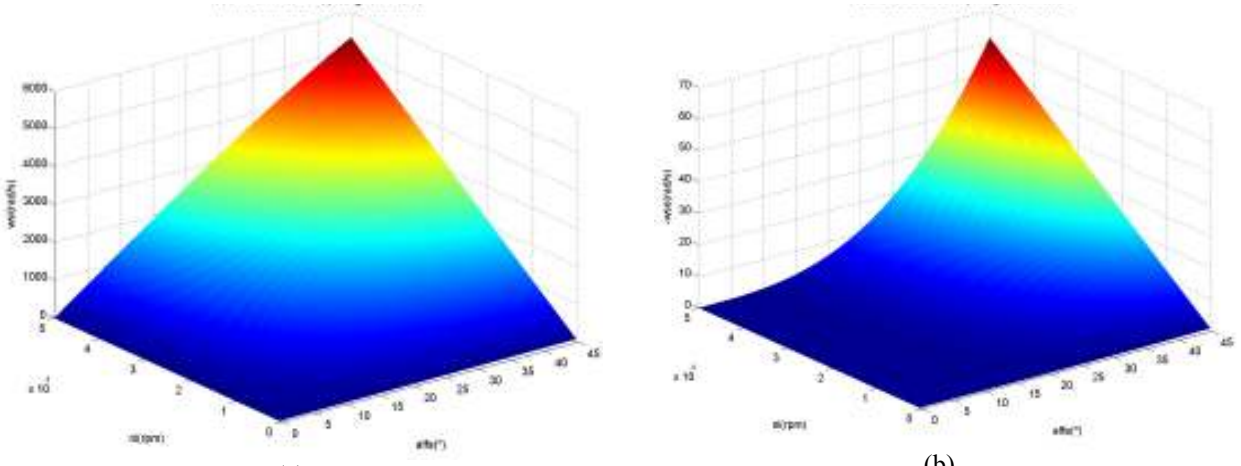

(a) (b)

Figure 8: Kinematic analysis: (a) Normal angular velocity at the inner contact; (b) Normal angular velocity at the outer contact

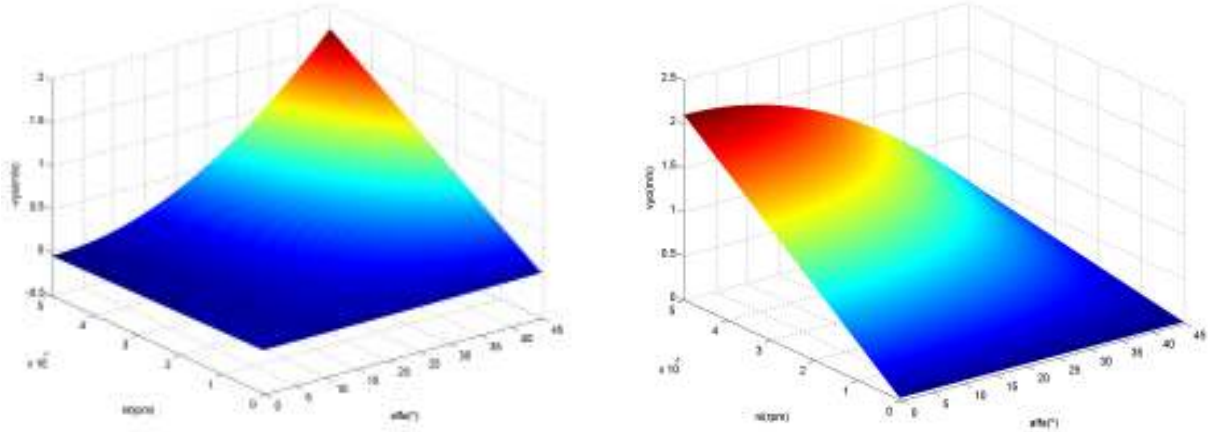

(a) (b)

Figure 9: Kinematic analysis: (a) sliding velocity at the outer raceway for $x_0 = 0$; (b) sliding velocity at the outer raceway for $x_0 = a_0$

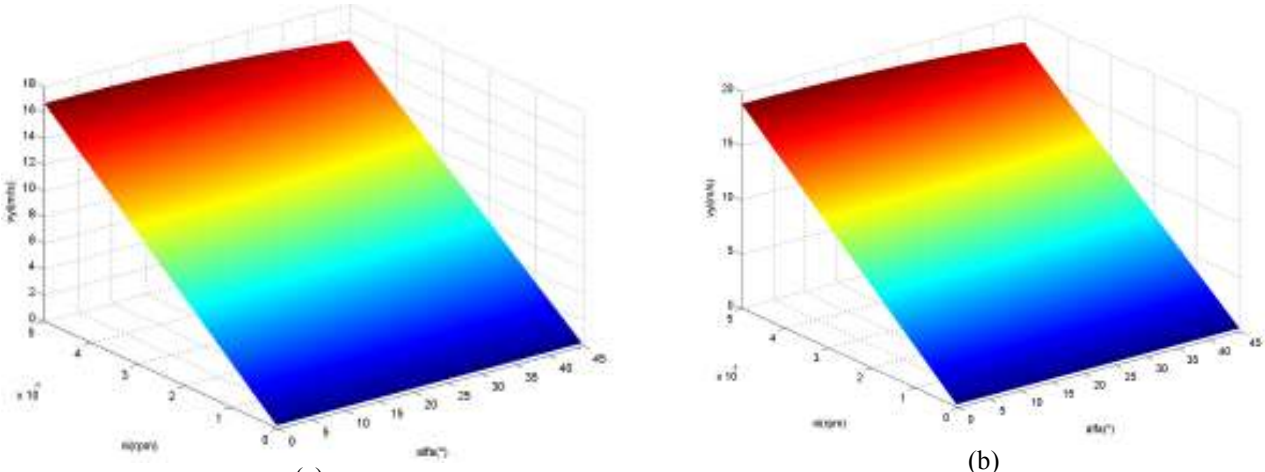

(a) (b)

Figure 10: Kinematic analysis: (a) sliding velocity at the inner raceway for $x_i = 0$; (b) sliding velocity at the inner raceway for $x_i = a_i$

At the same conditions, for 50.000 rpm, the inner raceway sliding velocity is 16,5 m/s at the contact center and 18m/s at the ellipse extremity. For normal rotations of 10.000 rpm, it is observed sliding velocities of 2 m/s at the contact center and 4m/s at the ellipse extremity (Figures 10(a) and 10(b)).

Finally, for the bearing analyzed here, the inner raceway sliding velocity, for usual applications, reaches next to 7% from the linear velocity at the ball surface.

3.3 Sensitivity analysis of the β angle

Figures 11(a) and 11(b) show the effect of α e β, in a range from 0° to 45°, considering the normal velocities (spinning) at the outer raceway contact areas, while Figures 12(a) and 12(b) consider the inner raceway. In both cases, there is a β angle in which the spinning is null, and the outer raceway control effect is obtained. Figure 11 (b) gives the curve for a bearing contact angle α of 30°, at which ω_{so} is null for β equal to 25,625°. At the same condition, there is also a β angle where ω_{si} is null (Figure 12(b)), around 40°, which is a very high value, not feasible to angular contact bearings operation.

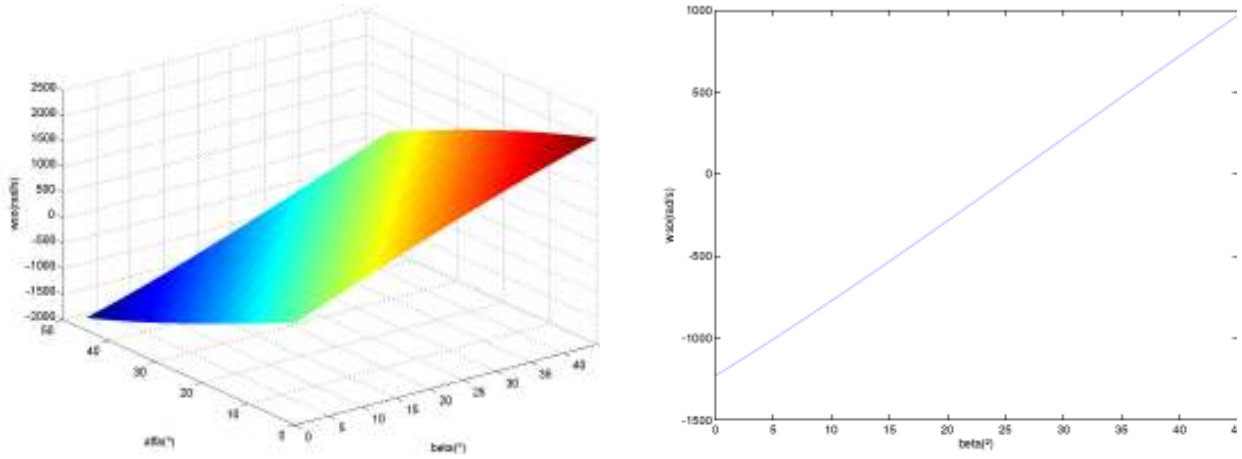

(a) (b)

Figure 11: Sensitivity analysis: (a) normal angular velocity at the outer ring contact;
(b) normal angular velocity at the outer ring contact for α=30°

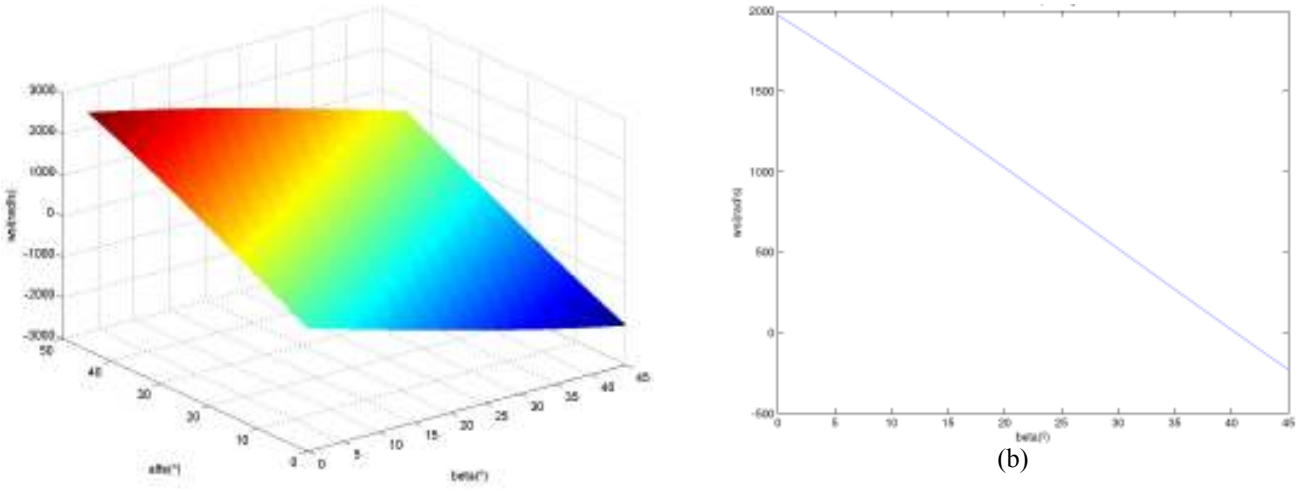

(a) (b)

Figure 12: Sensitivity analysis: (a) normal angular velocity at the inner ring contact;
(b) normal angular velocity at the inner ring contact for α=30°

4 CONCLUSIONS

Several operation conditions were simulated to analyze the kinematics of the angular contact bearing components and, consequently, their influence on the rolling elements loads.

The kinematic analysis focused the inner raceway rotation and the contact angle effects, considering their influence on the spinning and the sphere sliding velocities. The inner ring rotation is directly proportional to the sphere and the retainer velocities. The contact angle causes considerable effects on the sliding velocities at the contact zones between the sphere and the inner and outer raceways, generating increased sliding (up to 7% of the linear velocity at the sphere surface) at the inner raceway contact. The kinematic analysis is in agreement with the outer raceway control.

An important conclusion from the results is the expressive difference between the normal angular velocities to the inner and outer raceway contact. This difference has directly influence at the friction forces. For angular contact

bearings, at high rotation speeds, there is a change in the resultant forces equilibrium, due to the gyroscopic moment. This effect must be considered in the rolling elements loads, regarding the EHD lubrication condition.

The β angle in which the spinning is null, giving the outer raceway control condition, validates the method according the previous results obtained in the literature (HARRIS and KOTZALAS, 2006).

The simulation allows the foreseeing of the design parameters regarding the load distribution, which influences the fatigue life of the bearing.

Finally, the model is promising to estimate accelerations and velocities present in the rolling elements, factors that are strongly connected to the lubrication condition.

5 ACKNOWLEDGEMENTS

The authors appreciate and thank the research funds from Fapesp, CAPES and CNPq, as well as the Schaeffler Brasil Ltda. for the technical support to this paper.

6 REFERENCES

CHANGQING, B., 2006, "Dynamic model of ball bearings with internal clearance and waviness", Journal of Sound and Vibration, Vol. 294, pp. 23–48.

CHANGSEN, W., 1991, "Analysis of Rolling Element Bearings". London: Mechanical Engineering Publications LTD., 411p.

GOODMAN, J., 1912, "Roller and Ball Bearings", Proceedings of the Institute of Civil Engineering, Vol. 189 pp. 82–166.

GUPTA, P. K., 1979, "Dynamics of rolling element bearings part III: Ball bearing analysis", ASME Journal of Lubrication Technology, Vol.101, pp.311-326.

HAGIU, G.D., 1997, "Dynamic characteristics of high speed angular contact ball bearings", Wear, Vol. 211. pp. 22-29.

HARRIS, T.A., 1991, "Rolling Bearing Analysis". New York: John Wiley & Sons, 1011p.

HARRIS, T.A.; KOTZALAS, M.N., 2006, "Advanced Concepts of Bearing Technology". 5ª edição, Florida-USA: CRC Press, 342p

LIAO, N.T., 2002, " Ball bearing skidding under radial and axial loads", Mechanism and Machine Theory**.** Vol. 37, pp. 91-13.

MEEKS, C. R., TRAN, L., 1996, " Ball bearing dynamic analysis using computer methods-part I: Analysis", ASME Journal of Tribology, Vol.118, pg.52-58.

NONATO F., 2009, "Modelo dinâmico para o contato em mancais de elementos rolantes sujeito à lubrificação elastohidrodinâmica", Master Dissertation (in portughese), Unicamp.

6. RESPONSIBILITY NOTICE

The authors are the only responsible for the printed material included in this paper.